Vol 16 No 12, December 2007
1009-1963/2007/16(12)/3798-05
Chinese Physics
© 2007 Chin. Phys. Soc.
and IOP Publishing Ltd

First-principles study on the electronic structure and optical properties of $Tl_2Cd_2(SO_4)_3$ and $Rb_2Cd_2(SO_4)_3$*

Xu Bin(徐 斌)[a] Cheng Zheng–Ze(程正则)[a)b)†], Yi Lin(易 林)[a], and Cheng Ze(成 泽)[a]

[a] *Department of Physics, Huazhong University of Science and Technology, Wuhan* 430074, *China*

[b] *Department of Physics, Xianning College, Xianning* 437005, *China*

(Received 22 March 2007; revised manuscript received 3 May 2007)

With the help of ab initio full-potential linearized augmented plane wave (FPLAPW) method, calculating the electronic structure and linear optical properties is carried out for $XCd_2(SO_4)_3$ (X =Tl, Rb). The results show that $Tl_2Cd_2(SO_4)_3$ (TlCdS) has a larger band gap than $Rb_2Cd_2(SO_4)_3$ (RbCdS) and the energy bands for RbCdS are more dispersive than those of TlCdS. From their partial densities of states (PDOS), we have observed that the hybridization between S ionic 2p and O atomic 2p orbitals forms SO_4 ionic groups. The remarkable difference between RbCdS and TlCdS is, however, the degree of hybridization between cation (Tl and Rb) and its surrounding oxygen atoms. In the view of quantum chemistry, the strong p-d hybridization indicates the existence of their cation ionic bonds (Cd-O, Rb-O, and Tl-O). The calculations of TlCdS and RbCdS show their optical properties to be less anisotropic. Their anisotropies in the optical properties mainly occur in a low photon energy region of 5–16 eV.

Keywords: langbeinite, electronic structure, band gap, optical properties
PACC: 7115A, 7120H, 7790

1. Introduction

The langbeinite family of sulfate with the general formula $A_2B_2(SO_4)_3$ has aroused much interest because of their ferroelastic and ferroelectric behaviours as well as structural transition.[1] Among these are the archetype cubic mineral langbeinite $K_2Mg_2(SO_4)_3$, which is optically active in point group $P2_13$. A moderate electro-optic effect has been measured in several isomorphs.[2−4] Ferroelectric activity in $(NH_4)_2Cd_2(SO_4)_3$ was first reported in 1956[5] and confirmed later, and it was also demonstrated in TlCdS.[6,7] A number of the langbeinites have the common characteristic of high temperature cubic structure and undergo transitions to ferroelastic and sometimes also ferroelectric.[8] In general, they can be classified into two basic types in terms of their transition behaviours.[9,10] The first-type crystals exhibit multiple phase transitions from cubic ($P2_13$) to orthorhombic ($P2_12_12_1$) across two intermediates, monoclinic ($P2_1$) and triclinic ($P1$) phases such as RbCdS and TlCdS.[10] The second-type crystals undergo single phase transition from cubic ($P2_13$) to orthorhombic structure ($P2_12_12_1$).[11]

Experimental efforts have been made to investigate phase transitions of TlCdS and RbCdS.[12,13] The detailed crystal structures of TlCdS and RbCdS were determined by x-ray diffraction.[14,15] For cubic ($P2_13$), monoclinic ($P2_1$) and orthorhombic ($P2_12_12_1$) phases, the transition temperatures of TlCdS are 293, 121, 85 K, respectively[12,14] and those of RbCdS are 298, 120 and 85 K, respectively.[15] To the best of our knowledge, there are few ab initio calculations for electronic structure and optical properties of paraelectric TlCdS and RbCdS due to the complexity of crystal structures.

The aim of this paper is to theoretically investigate the electronic energy band, total densities of states (DOS), partial densities of states (PDOS) and optical properties for the TlCdS and RbCdS, based on the full potential linearized augmented plane wave (FPLAPW) method. The rest of this paper is organized as follows: we explain the computational method in Section 2; The computation results are shown in Section 3 for the electronic structure and optical properties; Finally, we draw some conclusions

*Project supported by the National Science Foundation of China (Grant No 2006CB921605) and the National Natural Science Foundation of China (Grant Nos 10174024 and 10474025).
†E-mail: czz8986@126.com

from this study in Section 4.

2. Computational details

The calculations presented in this paper are performed within the generalized gradient approximation[16] to the density functional theory as implemented in the WieN2K compute code,[17] using the FPLAPW method. In this method no shape approximation to either potential or the electronic charge density is made. We use Wien2K implementation of the method, which allows including local orbits in the basis, improving linearization and making possible a consistent treatment of semicore and valence states in one energy window, hence ensuring proper orthorhombicity. In the FPLAPW method, the unit cell is divided into two parts: (1) non-overlapping atomic spheres (centred at the atomic sites) and (2) an interstitial region. In the orthorhombic phase of TlCdS, the lattice parameters $a = 10.327$ Å, $b = 10.345$ Å, $c = 10.406$ Å[14] and the atomic sphere radii 2.9, 3.0, 1.5 and 1.2 respectively for Tl, Cd, S and O are used in our calculation. For the orthorhombic phase of RbCdS, the lattice parameters we $a = 10.319$ Å, $b = 10.321$ Å, $c = 10.320$ Å[15] and the atomic sphere radii 2.9, 3.0, 1.5 and 1.2 respectively, for Rb, C, S and O are used, in our calculation. The convergence parameter $RK_{\max}$ ($R_{\mathrm{mt}} \times K_{\max}$, where $K_{\max}$ is the plane-wave cut-off and R_{mt} is the smallest among all atomic sphere radii), which controls the size of the basis sets in these calculations, is set to be 8.0. We use $4 \times 4 \times 4$ meshes, which represent 80 k-points in the first Brillouin zone (BZ).

Because the dielectric function mainly pertains to the electronic response, our calculated optical properties will be helpful to an understanding of the different electronic structures for TlCdS and RbCdS. Adopting the one-electron, rigid band approximation, neglecting electron polarization effects (Koopmans approximation) and in the limits of linear optics and of the visible-ultraviolet region,[18,19] the imaginary part of a matrix element of the dielectric tensor is given by

$$\varepsilon_2(\omega) = \Big(\frac{4\pi^2 e^2}{m^2\omega^2}\Big) \sum_{i,f} \int_{\mathrm{BZ}} \frac{2\mathrm{d}k}{(2\pi)^3} |\langle \varphi_{fk}|e \cdot p|\varphi_{ik}\rangle|^2 \times \delta(E_{\mathrm{f}}(\omega) - E_i(\omega) - \hbar\omega) \quad (1)$$

for a vertical transition from a filled initial state $|\varphi_{ik}\rangle$ of energy $E_i(k)$ to an empty final state $|\varphi_{fk}\rangle$ of energy $E_{\mathrm{f}}(k)$, with wave vector k. Here ω is the frequency, e the electron charge, m the free electron mass, and p the momentum operator.

3. Results and discussion

Since the optical spectra are calculated from interband transitions, it is of interest to first describe our calculated electronic structure. For this reason, the calculated band structures and total DOS for TlCdS and RbCdS along the high-symmetry lines of the BZ are shown in Figs.1(a) and 1(b), respectively, where the zero of energy is chosen to coincide with the top of the valence band on the analogy of Wang *et al*'s treatment in Ref.[20], where studied is the energy band of insulating cubic perovskite. For TlCdS, the calculated band gap of 3.99 eV is an indirect gap. The bottom of the conduction band (CB) is at a point along $\Gamma - \Delta$ close to Γ, and the top of the valence band (VB) is at X. The direct gap at Γ is 3.992 eV. For RbCdS, we obtain a direct band gap of 3.694 eV at Γ, which is about 0.284 eV smaller than that of TlCdS. It is noted that the calculations in the local density function approximation have a difference in band gap between the theoretical predictions and experimental measurements, and the resulting narrower theoretical band gap is a well-known artifact of the local density approximation and it usually dose not have a significant effect on the rest of the band structure.[21] Figure 1 shows a comparison between the band structures of TlCdS and RbCdS. The two band structures are alike in general feature in that their crystal structures are similar. However, from the band structures, we can remark that the energy bands of RbCdS are more dispersive than those of TlCdS.

Figure 2 shows the partial DOS of TlCdS and RbCdS. It is clear that the SO_4 ionic groups mainly come from the hybridization between S ionic 2p and O atomic 2p orbitals. In Fig.2(a), the valence bands are derived mainly from Cd 5s, Tl 6s, S 2p and O (1, 2) 2p states from about –8 eV up to the Fermi level. The DOS of Tl 6s is similar to that of O 2p, which shows that the O 2p orbitals are strongly hybridized with Tl 6s orbitals. By comparing with Fig.2(b), we observe that the DOS of Tl 6s is little similar to that of O 2p. And it is also found that even though the DOS of Cd 5s is lower than that of O 2p, they are very much alike. This reflects that some electrons in the Cd 5s transform from conduction band into valence band and take part in the weak interaction between Cd and O, which is the same as the interaction between Cd

and O in Fig.2(b). The contribution of other states is at least one order of magnitude smaller. In Fig.2 we can see that PDOS of Tl atom have higher peaks than those of Rb atom, which shows that the interaction between Tl 6s and O 2p orbitals is stronger than between 5s states of Rb atom and 2p states of O atom below the Fermi level.

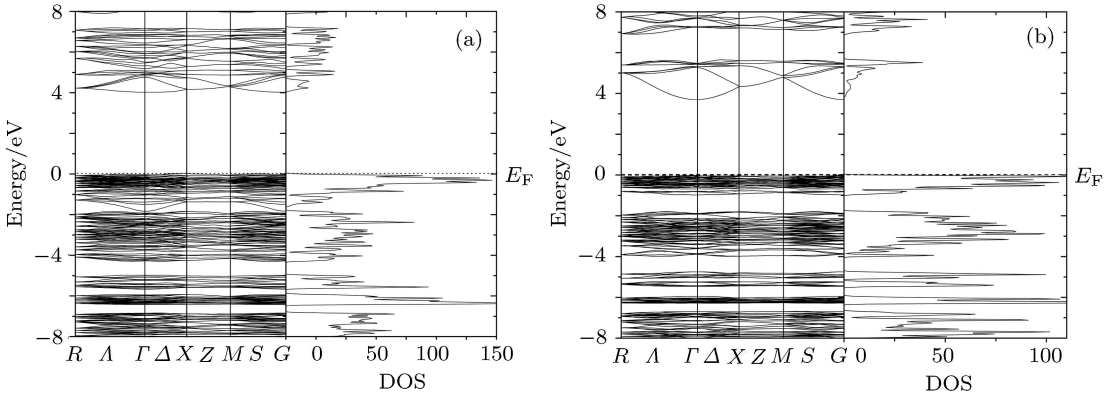


Fig.1. Band structures and the total densities of states for TlCdS(a) and RbCdS(b).

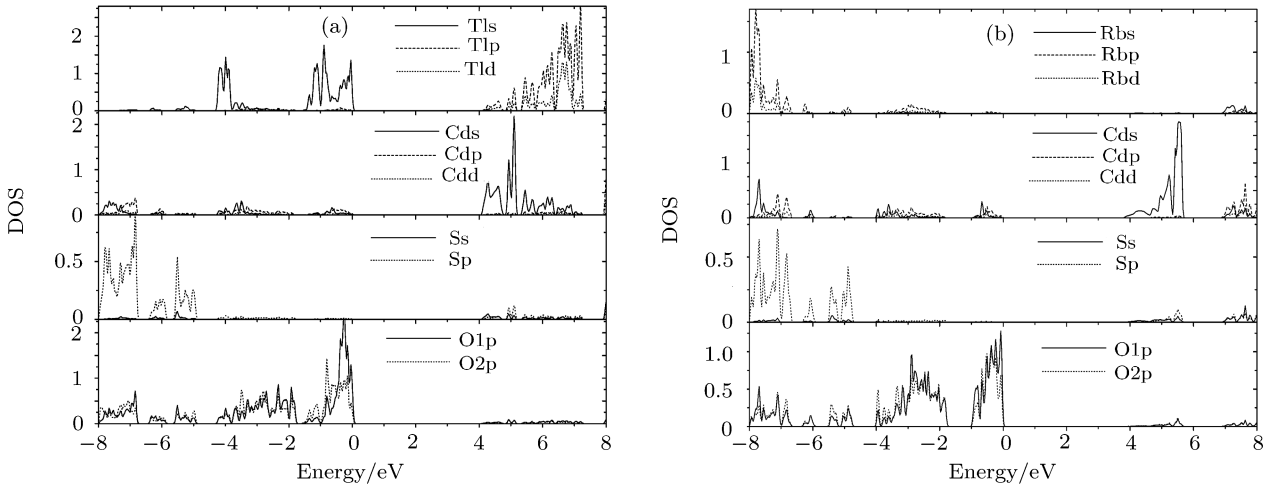


Fig.2. Partial densities of state for TlCdS (a) and RbCdS (b).

For TlCdS, the conduction bands are composed mainly of 6p states of Tl atom, 5s states of Cd atom, and 2p states of O atom. However, for RbCdS, the conduction bands are comprised mainly of 5s states of Cd atom and 2p states of O atom. It is very interesting that the DOS of S 2p are almost the same as those of O 2p from 5 to 7 eV, which implies that the hybridization between S ionic 2p and O atomic 2p orbitals forms SO_4^{2-}. Meanwhile we also observe that the hybridization between S ionic 2p and O atomic 2p orbitals forms SO_4^{2-} in Fig.2(b). One remarkable difference in hybridization between RbCdS and TlCdS is, however, the degree of hybridization between cation (Tl and Rb) and its surrounding oxygen atoms. Meanwhile, Cd, Tl and Rb atomic 4d orbitals have hybridized with O atomic 2p orbitals, resulting in the cation valence-ionic bonds, where the combination of Cd and O atoms are dominant. In view of quantum chemistry, the strong p-d hybridization indicates the existence of their cation ionic bonds (Cd-O, Rb-O, and Tl-O).

It has been earlier found that the calculated optical properties and electronic structures for $Zn_{1-x}Co_xX$ (X=S,Se,Te),[22] Fe nanowires on Cu(001) and Ag(001)[23] and TiO_2[24] are in excellent agreement with the experimental findings, and we have therefore used the same theory to predict the optical properties of TlCdS and RbCdS. Since the optical spectra are obtained from the interband transitions, the peak structures in Fig.3 can be explained through

our band structure. To our knowledge, there exist no experimental data concerning the dielectric function for both TlCdS and RbCdS. Figure 3 shows our calculated dielectric function in a photon energy range of up to 27 eV. The anisotropic features of these functions are demonstrated by their differences along the crystallographic a, b, and c axes, separately. However the general features of the dielectric functions of TlCdS and RbCdS appear to be similar along the three directions. Subtle differences in the structure can be identified. The anisotropies in the optical properties of TlCdS and RbCdS occur mainly at a low photon energy region of 5–16 eV. As there should be one-to-one correspondence between band structure and optical spectrum, we look first at the imaginary part of the optical dielectric tensor $\varepsilon_2(\omega)$.

For TlCdS, the lowest-energy peak at 5.85 eV in the $\varepsilon_2(\omega)$ spectra along the a, b and c axes arises from the interband transition between the valence band in –2.1 eV and the bottommost conduction band. The energy peak at 7.65 eV is due to interband transition from the band in –3.96 eV to the bottommost conduction band. For RbCdS, the lowest-energy peak around 5.5 eV in the $\varepsilon_2(\omega)$ spectra along the a, b and c axes arises from the interband transition between the valence band in –1.53 eV and the bottommost conduction band. Around 6.8 eV a sharp peak appears in all the three directions. The origin of this peak is due to the interband transitions from the band in –2.83 eV to the bottommost conduction band. The energy peak around 9.2eV is due to the interband transitions from the band in –5.23 eV to the bottommost conduction band. The peaks in the $\varepsilon_2(\omega)$ spectra above 8 eV, visible in all the three directions, are broad and involve several bands.

The imaginary part of the optical dielectric tensor $\varepsilon_1(\omega)$ is shown in Fig.3. The $\varepsilon_1(\omega)$ is obtained from $\varepsilon_2(\omega)$ using the Kramers–Kronig analysis. The $\varepsilon_1(0)$ value for RbCdS (TlCdS) from our calculations is about 2.3 (2.89). The sign changes occur in the $\varepsilon_1(\omega)$ spectra about at 5.55, 7.33, 8.82 eV for RbCdS and at 4.44, 6.27 eV for TlCdS along the three directions and they appear at the same energy as a peak in the corresponding $\varepsilon_2(\omega)$ spectra. Since in this range the imaginary part of the dielectric function is very low, the conditions for a plasma resonance are satisfied.

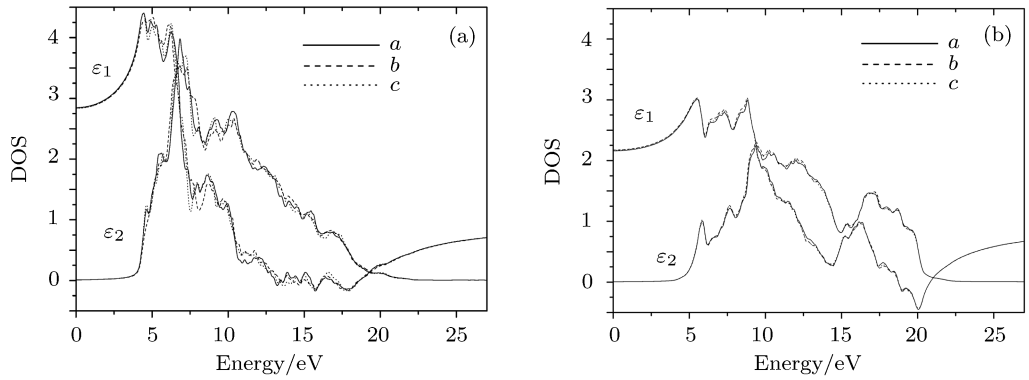


Fig.3. Real and imaginary parts of the dielectric functions for TlCdS (a) and RbCdS (b).

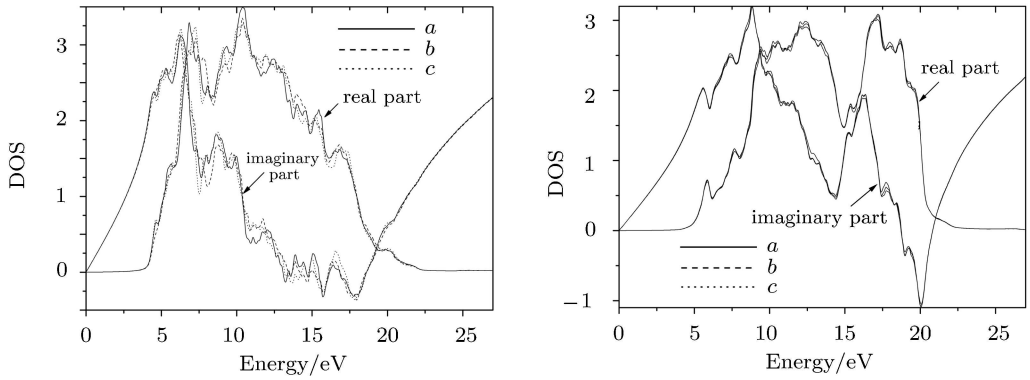


Fig.4. Real and imaginary parts of the optical conductivities for TlCdS (a) and RbCdS (b).

The real and the imaginary parts of the optical conductivity are shown in Figs.4(a) and 4(b) for TlCdS and RbCdS along the crystallographic a, b, and c axes in an energy range of 0–27 eV, respectively. Since there exist no experimental data available, we are not to discuss the optical conductivity here.

4. Conclusions

We present detailed calculations of the structural, electronic and optical properties of orthorhombic TlCdS and RbCdS using the FP-LAPW method. The general features of the two band structures are alike in that their crystal structures are similar. Our results show that RbCdS has a larger band gap than RbCdS, and it has more dispersive valence bands and conduction bands than TlCdS. It is clear that the SO_4 ionic groups mainly come from the hybridization between S ionic 2p and O atomic 2p states. The difference in electronic property is due to the differences in both crystal structure and local shortrange order between the two crystals. In the view of quantum chemistry, the strong p-d hybridization indicates the existence of their cation ionic bonds (Cd-O, Rb-O, and Tl-O). The calculations of optical properties for RbCdS and TlCdS show the optical properties to be less anisotropic, and reflect their differences in electronic structure. The anisotropy in the optical properties of TlCdS and RbCdS occurs mainly in a low photon energy region of 5–16 eV. Furthermore, the origin of the different optical properties between the two materials has been discussed. In addition, we have examined the optical conductivities. We have not found any published data about the electronic structure and optical properties of orthorhombic TlCdS and RbCdS, so our calculations can be used to cover the lack of data for these compounds.

References

[1] Zemann A and Zemann J 1957 *Acta Crystallogr.* **10** 409.
[2] Buhrer C F and L Ho 1964 *Appl. Opt.* **3** 314
[3] Fmmenegger E, Nitsche R and Miller A 1968 *J. Appl. Phys.* **39** 3039
[4] [4] Ivanov N R and Koniak C 1975 *Sov. Phys. Crystallogr.* **19** 755
[5] Jone F and Pepinsky R 1956 *Phys. Rev.* **103** 1126
[6] Brezina B and Glogarova M 1972 *Phys. Status Solidi A* **11** 39
[7] Glogarova M, Fousek J and Brezina B 1972 *J. Phys.* C **33** 2
[8] McMurdie H F, Morris M C and DeGroot J 1971 *J. Res. Natl. Bur. Stand.* **75** 435
[9] Brezina B and Glogarova M 1972 *Phys. Status Solidi* A **11** K39
[10] Abrahams S C, Lissalde F and Bernstein J L 1978 *J. Chem. Phys.* **68** 1926
[11] Noboru Y, Masaki M and Hideaki A 1981 *J. Phys. Soc. Jpn.* **50** 907
[12] Cao H, Dalley N K and Goates J B 1993 *Ferroelectrics.* **146** 45
[13] Hikita T, Kudo T and Chubachi Y 1976 *J. Phys. Soc. Jpn.* **41** 349
[14] Guelylah A, Madariaga G, Morgenroth W, Aroyo M L, Breczewski T and Bocanegra E H 2000 *Acta Cryst.* B **56** 921
[15] Nalini G and Guru R T N 2002 *Chem. Mater.* **14** 4729
[16] Perdew J P, Chevary J A, Vosko S H, Jackson K A, Perdoson M R, Singh D J and Fiolhais C 1992 *Phys. Rev.* B **46** 6671
[17] Blaha P, Schwarz K, Madsen G K H, Kvasnicka D, Luitz J, WIEN2K, Vienna University of Technology 2002, Improved and Updated UNIX Version of the Original Copyrighted WIENCODE, which was published by Blaha P, Schwarz K, Sorantin P and Trickey S B 1990 *Comput. Phys. Commun.* **59** 399
[18] Lynch W D, in: E. D. Palik (Ed.) 1985 *Handbook of Opticals Constants of Solids* (New York: Academic Press)
[19] Bassani F, Parravicini G P and Ballinger R A 1975 *Electronic States and Optical Transitions in Solids* (Oxford: Pergamon)
[20] Wang Y X, Zhong W L, Wang C L and Zhang P L 2001 *Phys. Lett.* A **291** 338
[21] Jones R O and Gunnarsson O 1989 *Pre. Mod. Phys.* **61** 689
[22] Ouyang C Y, Xiong Z H, Ouyang Q Z, Liu G D, Ye Z Q and Lei M S 2006 *Chin. Phys.* **15** 1585
[23] Jin Y J,Li Z Y and Lin J B 2007 *Chin. Phys.* **16** 506
[24] [24] Peng L P, Xu L and Yin J W 2007 *Acta Phys. Sin.* **56** 1585